The Formation of Se_2^-: A New Resonance Raman Feature in the Photochemistry of Zeolite-Encapsulated Selenium

Andreas Goldbach, Lennox Iton, Marcos Grimsditch, and Marie-Louise Saboungi*

Contribution from Argonne National Laboratory, Argonne, Illinois 60439

Received September 18, 1995[⊗]

Abstract: This Raman spectroscopic study on selenium incorporated in Nd−Y zeolite presents new aspects of the photochemistry of selenium. The formation of the Se_2^- radical anion has been established from its resonance Raman spectrum, consisting of ten almost equidistant bands between 328 and 3220 cm^{-1} on the low-energy side of the 476.24-nm laser excitation line. The derived spectroscopic constants of the electronic ground state are $\omega_0 = 328$ cm^{-1} and $x_0\omega_0 = 0.71$ cm^{-1}. Another broad band at 260 cm^{-1} resembles features in the Raman spectra of amorphous selenium and selenium chain structures encapsulated in zeolites. Continuous irradiation at sufficiently high laser power levels leads to depletion of the 260 cm^{-1} band and a simultaneous enhancement of the Se_2^- bands. These observations are discussed with respect to the defect states conventionally invoked for reversible photoinduced changes in amorphous selenium.

Introduction

Selenium has been loaded into a variety of molecular sieves like mordenite, faujasites (X, Y), zeolite A, and $AlPO_4$-5 in order to study the influence of spatial confinement on its structure, using various techniques ranging from diffraction by X-rays[1] and more recently by anomalous X-ray scattering,[2] extended X-ray absorption fine structure (EXAFS),[3−6] and Raman spectroscopy.[1,7−10] The structural picture shows basically one-dimensional Se chains occupying the voids in the molecular sieves. Only for zeolite A do the experimental results support the formation of isolated clusters like Se_8 rings.[6,9] In one-dimensional channel systems like mordenite or $AlPO_4$-5 the Se chains are isolated, highly ordered helical structures.[3−6,8,11] The three-dimensionally linked large pores of the zeolites X and Y impose less rigid constraints on the Se chains. Thus, it is possible that more than one Se chain can occupy the same cage and that irregular chain bending causes deviations from the regular helical conformation.[6,12]

Electronic absorption spectra show clearly that the properties of Se incorporated in zeolite A[6,12,13] differ essentially from those in the other molecular sieves. In the case of zeolite A, the absorption spectrum is closely related to that of bulk monoclinic Se which consists of Se_8 rings.[6,12] However, in several Y and X zeolites, as well as in mordenite and $AlPO_4$-5, the spectra are analogous to that of trigonal Se which is composed of helical chains.[6,12] In general, a blue shift of the band gap is observed with respect to the band gaps of bulk monoclinic (2.53 eV) and trigonal Se (1.98 eV).[6]

Zeolites-encapsulated Se are photosensitive.[5,7] After illumination with visible light of various wavelengths at low temperatures, new bands appear in the absorption spectra. It is likely that these changes in the optical behavior are accompanied by structural modifications of the selenium. In addition to the photoinduced spectral bands, the formation of paramagnetic centers has been established by ESR spectroscopy following illumination.[5] However, these species have not been well-characterized or convincingly identified.

We report Raman spectroscopic results obtained on Se loaded into a neodymium-exchanged Y zeolite. Whereas in the case of monovalent cations each supercage of the Y zeolite contains several metal ions, the Nd^{3+} cations only occupy the smaller β-cages. The absence of cations in the supercages can also be expected to influence the incorporation of Se into the zeolite. Besides the well-known chain structures, we are able to identify unambiguously the presence of Se_2^- radical anions, which have to our knowledge not previously been observed in zeolites. We discuss possible mechanisms for the formation of this radical anion.

Experimental Section

The Nd−Y zeolite was obtained by a 2-fold ion exchange of the Na−Y zeolite with a $Nd(NO_3)_3$ solution. It was dried by heating for 20 h under vacuum in several steps to 500 °C, followed by annealing at 550 °C under a static oxygen atmosphere for 4 h, and then evacuated at 550 °C for 20 h. After cooling under vacuum the zeolite was transferred to a glovebox and then loaded into one arm of a quartz U-tube. The two arms of the tube were separated by a quartz frit. Se sufficient to yield 10 Se atoms per supercage of the zeolite was loaded

[⊗] Abstract published in *Advance ACS Abstracts,* February 15, 1996.

(1) Bogomolov, V. N.; Efimov, A. N.; Ivanova, M. S.; Poborchii, V. V.; Romanov, S. G.; Smolin, Yu. I.; Shepelev, Yu. F. *Sov. Phys. Solid. State* **1992**, *34*, 916.

(2) Armand, P.; Saboungi, M.-L.; Iton, L.; Price, D. L. To be submitted for publication.

(3) Tamura, K.; Hosokawa, S.; Endo, H.; Yamasaki, S.; Oyanagi, H. J. *Phys. Soc. Jpn.* **1986**, *55*, 528.

(4) Endo, H.; Inui, M.; Yao, M.; Tamura, K.; Hoshino, H.; Katayama, Y.; Maruyama, K. *Z. Phys. Chem. N.F.* **1988**, *156*, 507.

(5) Katayama, Y.; Yao, M.; Ajiro, Y.; Inui, M.; Endo, H. *J. Phys. Soc. Jpn.* **1989**, *58*, 1811.

(6) Parise, J. B.; MacDougall, J. E.; Herron, N.; Farlee, R.; Sleight, A. W.; Wang, Y.; Bein, T.; Moller, K.; Moroney, L. M. *Inorg. Chem.* **1988**, *27*, 221.

(7) Bogomolov, V. N.; Poborchii, V. V.; Kholodkevich, S. V.; Shagin, S. I. *JETP Lett.* **1983**, *38*, 532.

(8) Bogomolov, V. N.; Poborchii, V. V.; Romanov, S. G.; Shagin, S. I. *J. Phys. C: Solid State Phys.* **1985**, *18*, L313.

(9) Bogomolov, V. N.; Poborchii, V. V.; Kholodkevich, S. V. *JETP Lett.* **1985**, *42*, 517.

(10) Poborchii, V. V. *J. Phys. Chem. Solids* **1994**, *55*, 737.

(11) Terasaki, O.; Yamakazi, K.; Thomas, J. M.; Oshuna, T.; Watanabe, D.; Sanders, J. V.; Barry, J. C. *Nature* **1987**, *330*, 6143; *J. Solid State Chem.* **1988**, *77*, 72.

(12) Nozue, Y.; Kodaira, T.; Terasaki, O.; Yamakazi, K.; Goto, T., Thomas, J. M.; Watanabe, D. *J. Phys.: Condens. Matter* **1990**, *2*, 5209.

(13) Bogomolov, V. N.; Lutsenko, É. L.; Petranovskii, V. P.; Kholodkevich, S. V. *JETP Lett.* **1976**, *23*, 482.

0002-7863/96/1518-2004$12.00/0

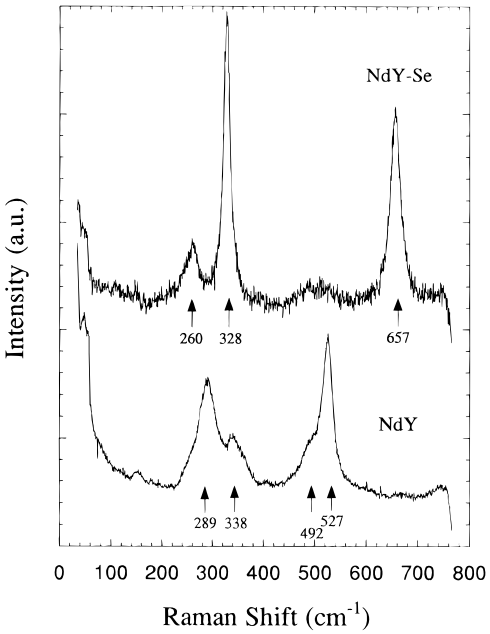

Figure 1. Raman spectra of the pure Nd−Y zeolite (lower trace) and the same zeolite loaded with 9.5 selenium atoms per supercage (upper trace). The arrows mark the positions of the main features.

into the second arm. The tube was sealed off at both ends under vacuum, placed into a furnace, and heated to 435 °C for 12 h. An orange colored powder was obtained in the zeolite-containing arm with traces of the elemental Se left in the other arm. The sample was annealed at 350 °C for 24 h for complete homogenization. From the weight balance it was calculated that 9.5 ± 0.6 Se atoms per supercage had been loaded.

The Raman spectra were measured at room temperature using a triple Jobin Yvon T64000 spectrometer equipped with an optical multichannel analyzer. Krypton ion laser radiation of wavelength 476.24 nm (20998 cm^{-1}) at maximum power of 100 mW was used for excitation. The resolution of the instrument was set to 6 cm^{-1}. A sample sealed in a quartz tube under vacuum was used for the measurements. The geometry of the CCD detection system limited the directly recorded range of the Raman spectrum to a maximum of 750 cm^{-1} from the excitation frequency. By adjusting the gratings, a spectrum covering a range of ∼5000 cm^{-1} could be assembled from 10 component spectra. Each individual spectrum was calibrated using the emission spectrum of a neon lamp. In order to compensate for intensity fluctuations of the laser radiation the shift of the detected spectral range was chosen so that adjacent spectra overlapped by at least 350 cm^{-1}.

Results

Figure 1 displays the Raman spectra of the both the pure and the Se-loaded Nd−Y zeolite up to 765 cm^{-1}. The spectrum of the pure zeolite shows three broad but clearly resolved bands at 289, 338, and 527 cm^{-1}, and a broad shoulder at 492 cm^{-1}. Raman bands around 300 and 500 cm^{-1} are characteristic of dehydrated faujasitic zeolites.[14] In the Se-loaded zeolite, these bands almost disappear and only the two features around 500 cm^{-1} are still weakly perceptible. Three new bands emerge: one rather broad and centered around 260 cm^{-1} and the other two quite narrow and an order of magnitude more intense at 328 and 657 cm^{-1}. While the feature at 260 cm^{-1} is characteristic of Raman bands reported for Se chains formed in some zeolites,[1,7,8,10] the other two bands have not been previously observed.

Figure 2 shows the Raman spectrum of the Se-loaded Nd−Y zeolite over a range of 5000 cm^{-1}. Eight new bands can be distinguished. Table 1 gives the positions of these bands as

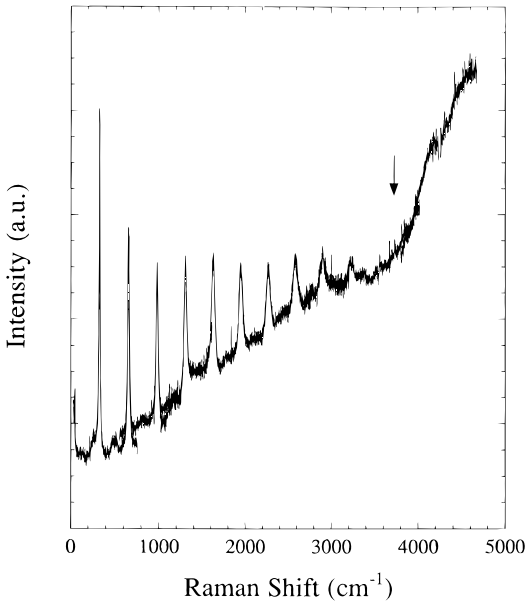

Figure 2. Raman spectrum of the selenium-loaded Nd−Y zeolite. The spectrum is dominated by the Se_2^- bands.

Table 1. Spectral Positions of the Observed Se_2^- Bands

band no. v	transition freq (cm^{-1})	Raman shift (cm^{-1})	band dist $v_n - v_{n-1}$ (cm^{-1})
1	20670	328.0	328.0
2	20341	656.8	328.6
3	20016	981.8	325.2
4	10692	1306.4	324.6
5	19372	1625.8	319.4
6	19051	1947.3	321.5
7	18730	2268.2	320.9
8	18413	2585.3	317.1
9	18097	2900.9	315.6
10	17779	3219.3	318.4

absolute transition frequencies, and the Raman shifts relative to the excitation frequency. A repeat measurement with a slightly higher excitation wavelength (482.52 nm) gave identical shifts for these lines identifying them as Raman scattering and not fluorescence. With increasing distance from the exciting line, these bands broaden significantly and a strong background is observed starting at ∼600 cm^{-1} and increasing steeply at about 3700 cm^{-1} (i.e. an absolute frequency of 17300 cm^{-1}).

As can be seen from both Figure 2 and Table 1 the sequence of these transitions is very regular and the spacing between successive bands decreases slightly with increasing Raman shift. This is characteristic of transitions between vibrational levels of different electronic states of molecules. Figure 3 shows a plot of spacings between consecutive bands versus an arbitrarily assigned vibrational quantum number v, i.e. the number of the band in Table 1 (Birge−Sponer plot). Using a linear fit to derive the spectroscopic constants of the electronic level involved, we obtained 328 cm^{-1} for the fundamental vibration frequency ω_0 and 0.71 cm^{-1} for the anharmonicity constant $x_0\omega_0$. These values agree with those reported for the electronic ground state of the $^{80}Se_2^-$ radical anion doped into a KI crystal, (328.5 ± 0.9) and (0.75 ± 0.04) cm^{-1}, respectively.[15] Hence, the identification of Se_2^- is unambiguous. Since the Raman shift of the first transition, 328 cm^{-1}, matches the reported value[16] for the fundamental vibration frequency, the assigned quantum numbers v must be the correct absolute numbers. The broadening of the Se_2^- bands with increasing Raman shift is

(14) Brémard, C.; Le Maire, M. *J. Phys. Chem.* **1993**, *97*, 9695.

(15) Rolfe, J. *J. Chem. Phys.* **1968**, *49*, 4193.

(16) Holton, W. C.; de Wit, M. *Solid State Commun.* **1969**, *7*, 1099.

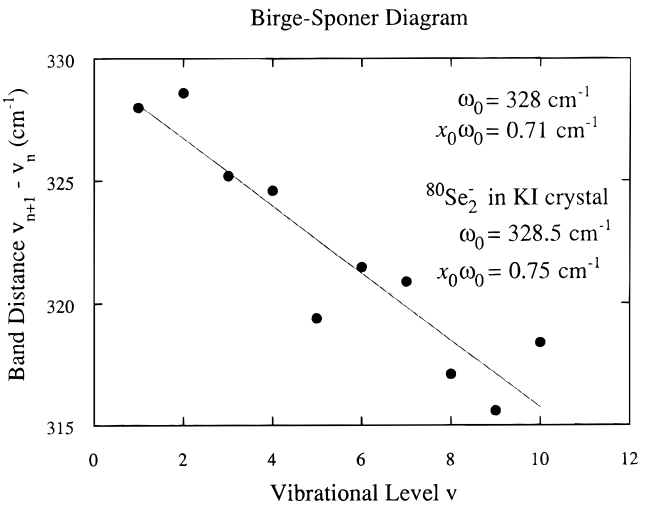

Figure 3. Birge−Sponer plot: The distances of subsequent bands are plotted versus the vibrational quantum numbers assigned to the bands. The line is a linear fit yielding the fundamental vibration frequency ω_0 and the anharmonicity constant $\omega_0 x_0$ of the electronic ground state (see text).

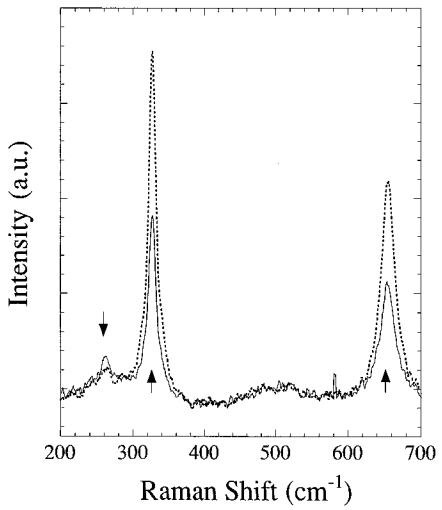

Figure 4. Influence of the 476.24-nm laser radiation on the spectral features. The solid line indicates a spectrum recorded directly after focusing the laser beam on the sample. The broken line spectrum was taken after 30 min of illumination. The Se_2^- bands (up arrows) grow under illumination while the selenium chain related band (down arrow) has decreased.

due to the use of natural Se in this experiment. Because Se is composed of six isotopes, 21 isotopic combinations for Se_2^- are possible and the resulting splitting of the energy levels is already quite large for $v = 10$.

The vibrational spectrum of Se_2^- in Figure 2 is clearly not a conventional Raman spectrum. We observe bands corresponding to overtone transitions with Δv as high as 10. Apart from the fact that such transitions are rather improbable, the strong intensities of the observed bands point to a special enhancement effect. We note also that each of the Se_2^- bands is much more intense than the band at 260 cm^{-1} arising from first-order scattering from the Se chains.

Obviously we are dealing with a resonance effect involving vibrational levels of two different electronic states. The frequency of the exciting radiation bridges precisely the energy gap between two particular rotational−vibrational levels of the Se_2^-, one belonging to the electronic ground state and the second to an excited electronic state. Thus the upper of these levels can be highly populated by the intense laser beam, and the excited radical anions decay back to the ground state emitting intense resonance radiation. Such a process is not subject to any selection rules on Δv. This scenario accounts for both the observed transitions and the high intensities. The actual concentration of Se_2^- may be small since its detection can be strongly favored by the advantageous resonance effect. (For example, in the case of gaseous Se_2, a resonance fluorescence spectrum has been observed that originates in the $v = 14$ vibrational level of the electronic ground state. Although the Boltzman factor for the occupation of this level at 500 °C is 4×10^{-5}, the signal-to-noise ratio was about 5000/1 for the strong lines.[17])

The excitation energy $hc\omega_{00}$ between the lowest vibrational levels in the ground and first excited electronic states for $^{80}Se_2^-$ in KI[15] is $\omega_{00} = 16011\ cm^{-1}$. This serves as a reference value, although the electronic excitation energy usually exhibits a substantially greater matrix dependence than the internal vibrational excitations, so that the corresponding value of ω_{00} could be quite different for the zeolite matrix. However, the highest energy emission band corresponds to a frequency of 20670 cm^{-1}, much higher than the reference value of ω_{00}. Therefore, the emission must be occurring from a high vibrational level, probably with $v > 15$, since the vibrational constant is expected to be smaller in the excited electronic state.

Figure 4 shows the time evolution of the Se-related bands in Figure 1. Continuous illumination of the sample with the probing radiation leads to an increase of the intensity of all the bands with the exception of the 260-cm^{-1} band representing the Se chains. At a laser output level of 100 mW these changes occur quite rapidly. In particular, the band representing the Se chains decreases drastically within minutes. The growth of the Se_2^- bands reaches a saturation level after 3 h and a weak trace of the 260-cm^{-1} feature remains. On the other hand, at an initial laser output level as low as 40 mW, the intensity of the 260-cm^{-1} feature is conserved for at least 1.5 h. The Raman bands corresponding to the zeolite itself become more prominent again. Evidently we are observing a photoinduced degradation of the Se chains with Se_2^- being one of the decomposition products. Since the Se_2^- bands do not decrease after suspending the irradiation of the sample for ∼2 h, the structural rearrangements are irreversible at room temperature on the time scale of our experiment.

Discussion

The decrease in intensity of the Raman band assigned to the selenium chains, in concert with the growth in intensity of the Se_2^- bands, supports the conclusion that Se_2^- anionic dimers are produced from longer Se chains by dissociation. However, the spectra obtained at low laser power confirm that Se_2^- anions are also present in the sample *before* its exposure to the radiation, implying that some Se_2^- is produced spontaneously in the zeolite under our conditions of preparation. The most likely source of these spontaneously produced anions is the neutral Se_2 dimer which is one of the predominant species present in the selenium vapor at the sample preparation temperature (435 °C). Some of the neutral dimers are apparently stabilized by reduction with an electron transferred from the zeolite instead of being incorporated into longer chains.

The fact that the dimeric species produced under irradiation is the anion suggests the occurrence of heterolytic bond breaking of the Se chains resulting in the formation of a shortened chain with a positively charged hole defect on the terminal Se atom

(17) Barrow, R. F.; Beattie, I. R.; Burton, W. G.; Gilson, T. *Trans. Faraday Soc.* **1971**, *67*, 583.
(18) Brabson, G. D.; Andrews, L. *J. Phys. Chem.* **1992**, *96*, 9172.

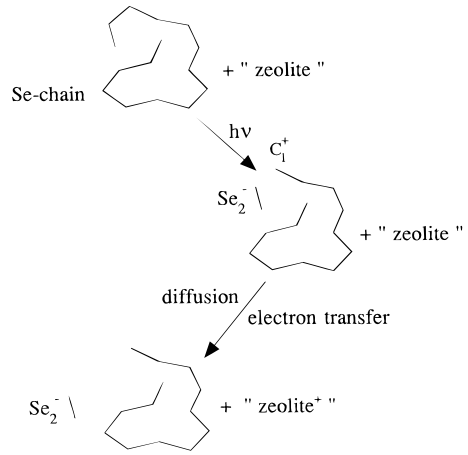

Figure 5. Reaction mechanism for the photoinduced formation of Se_2^- from chainlike Se. The notation of the involved atoms is described in the text.

(Figure 5). It has been demonstrated that the very high electrostatic fields found in the pores of zeolites are conducive to charge separation and the stabilization of ionic species.[19,20] In our case, heterolytic bond scission near the end of the chain generates a spin-paired C_1^+ defect on the remaining chain fragment and a Se_2^- radical anion. Since the dissociation is irreversible on the time scale of our experiments a stabilization of the initial ion pair must occur. The most plausible mechanism is the following. First, the Se_2^- diffuses from the immediate vicinity. Electron transfer from the zeolite to the accompanying C_1^+ defect then gives rise to a neutral chain end indistinguishable from the original chain end and creates a hole center in the zeolite host material. Subsequently the Se_2^- anion, which is an unpaired electron defect, is stabilized at this zeolitic hole center or another center generated in the same way.

It has previously been reported that photoinduced electronic absorption bands in isolated Se chains in zeolites appear around 1.85 (14920 cm^{-1}) and 2.15 eV (17340 cm^{-1}) upon irradiation *at low temperature* with radiation above the band edge.[5] These were also associated with the formation of paramagnetic defect centers as observed in the ESR spectrum.[5] The mid-gap centers were suggested to be uncharged dangling bond sites (C_1^0, the lower number denotes the bond coordination, the upper index the charge at the center) with unpaired electrons. We attach some significance to the fact that the onset of the increased fluorescence occurs at an absolute frequency of about 17300 cm^{-1} (Figure 3) which is identical to the position of the higher energy photoinduced electronic absorption band within the error limits.

Our results indicate that the photochemistry of short, isolated selenium chains is also different from the photochemistry of bulk amorphous Se. The latter is dominated by bond-switching processes between neighboring selenium chains, leading to an intrinsic C_1^- chain termination defect on one chain and a 3-fold bond-coordinated C_3^+ chain branching defect on the second chain. However for an isolated chain, interchain bonding to create the C_3^+ chain branching defect is not possible. Katayama et al.[5] attribute the photoinduced absorption in isolated Se chains in mordenite to paramagnetic C_1^0 defects formed by homolytic bond scission. Heterolytic bond scission far from the end of the chain would produce a diamagnetic C_1^- chain termination defect on one fragment and a corresponding diamagnetic C_1^+ hole defect on the terminus of the second chain fragment. This charge defect pair is unlikely to survive since the large chain fragments cannot diffuse apart at low temperature and will recombine. Instead, homolytic bond scission to yield two C_1^0 neutral defects, a lower energy defect pair, occurs in the mordenite. The pair of neutral (free radical) defects is thermally unstable and are annealed by rejoining the chain fragments when the mordenite is heated to 300 K.[5] For this reason, we do not believe that homolytic bond scission giving rise to neutral Se_2 that are subsequently converted to Se_2^- by electron transfer plays an important role here. In addition, we have no experimental evidence for the presence of the neutral dimer from the Raman spectrum.

Finally, an electron-transfer mechanism may also explain the spontaneous formation of Se_2^- prior to the illumination with the laser. Isolated trivalent Nd^{3+} ions are not reasonable candidates as electron donors since Nd^{4+} formation is not plausible. However, it is known that the exposure of zeolites ion-exchanged with polyvalent cations (e.g., La^{3+}, Ce^{3+}, Ti^{3+}) to molecular oxygen results in the formation of O_2^- analogous to Se_2^-.[21−23] We suggest that the reducing power of Nd^{3+}-substituted zeolite lies in the presence of oxide and/or hydroxide-bridged cation dimers or trimers in the sodalite cages which is confirmed by recent neutron diffraction measurements.[24] A plausible scenario involves the homolytic scission of the O−H bond of a bridging hydroxyl in the $[Nd_2(OH)_2]^{4+}$ cluster with the resulting hydrogen atom reducing the neutral Se_2 molecule and the unpaired electron stabilized on the cluster:

$$[Nd_2(OH)_2]^{4+} + Se_2 = [Nd_2(OH)(O)]^{4+} + Se_2^- + H^+ \quad (1)$$

Stabilization of the Se_2^- anions may be accomplished by the protons formed in (1). However, it should be noted that this reaction occurs at the temperature of preparation of the materials (435 °C) and therefore is not involved in the photolytic process at room temperature.[25]

Conclusion

The formation of the Se_2^- radical anion in a zeolite host has been reported for the first time. While the band at 260 cm^{-1} arises from first-order scattering from Se chains, the series of ten Se_2^- bands starting at 328 cm^{-1} results from a resonance Raman phenomenon. The evolution of both the Se_2^--related bands and the band originating from chain selenium under illumination with the laser radiation indicates a photoinduced decomposition of the Se chains with accompanying formation of Se_2^- fragments. Mechanisms are suggested that account for the irreversible formation of Se_2^- before and after irradiation with the laser.

Acknowledgment. This work was supported by the U.S. Department of Energy, Division of Materials Sciences, Office of Basic Energy Sciences, under Contract No. W-31-109-ENG-38. We thank Prof. F. Hensel for his interest in this work and A.G. acknowledges support by a research grant from the Deutsche Forschungsgemeinschaft.

JA9531788

(19) Kasai, P. H.; Bishop, R. J., Jr. *J. Phys. Chem.* **1973**, *77*, 2308.
(20) Rabo, J. A.; Kasai, P. H. *Prog. Solid State Chem.* **1975**, *9*, 1.
(21) Wang, K. M.; Lunsford, J. H. *J. Phys. Chem.* **1971**, *75*, 1165.
(22) Ono, Y.; Suzuki, K.; Keii, T. *J. Phys. Chem.* **1974**, *74*, 218.
(23) Krzyzanowski, S.; *J. Chem. Soc., Faraday Trans. 1* **1976**, *72*, 1573.
(24) Armand, P.; Iton, L. E.; Richardson, J.; Price, D. L.; Saboungi, M.-L. To be submitted for publication.
(25) We have verified that the heating produced by the laser is not significant. Raising the laser output level from 40 to 100 mW does not affect the position of the Se_2^- bands at 328 and 657 cm^{-1}. Furthermore, we have been able to measure in the same setup the Raman of amorphous Se even though its glass transition temperature is only 41 °C.